Research on Calculating Activities from Binary Phase Diagrams of Ti-Bearing Blast Furnace Slag

Chunling Yao [1, 2], Zhennan Liu [1, 2, *], Cong Liu [1], Ying Sun [1] and Yadong Li [1, 2]

[1] Faculty of metallurgy and mining, Kunming Metallurgy College, Kunming, China

[2] Kunming Key Laboratory of Comprehensive Utilization Resources of Rare and Precious Metals, Kunming, China

* Corresponding author: realsouth@126.com

Abstract. Based on Kuo-chih Chou formulae of calculating activities from binary phase diagrams, some methods are proposed to improve numerical integration for the formulae. The component activity data of CaO-SiO_2, MgO-SiO_2 and MnO-TiO_2 melts are calculated by the methods under the condition of regular solution's assumption. The calculation results are in reasonable agreement with experimental data, and the average relative errors between calculated values by using the methods and experimental data are 18%, 18% and 11% respectively. This accuracy is within experimental error range of 10%~30% that Turkdogan proposed. The results show that the new methods are feasible in the practical application. Accordingly, the component activity data of CaO-TiO_2, Al_2O_3-TiO_2, SiO_2-TiO_2 and MgO-TiO_2 melts at a given temperature and concentration are calculated by the proposed methods. The relative errors for these systems are comparable to the results of CaO-SiO_2, MgO-SiO_2 and MnO-TiO_2 systems. So the activity data obtained can be used as basic data for thermodynamic study of Ti-bearing blast furnace slag.

Keywords: Ti-bearing blast furnace slag, binary phase diagram, activity calculation.

1. Introduction

The main components of Ti-bearing blast furnace slag are CaO, Al_2O_3, SiO_2, MgO and TiO_2. The component activity data of their binary systems, CaO-TiO_2, Al_2O_3-TiO_2, SiO_2-TiO_2 and MgO-TiO_2, are essential in thermodynamic studies for the quinary system. However, the related thermodynamic studies of these four binary slag systems are seldom, and the corresponding binary activity data have not been reported at home and abroad. Since experimental determination of activity of slag system is difficult, it is of great scientific significance to take advantage of the limited thermodynamic data to estimate the activity of binary system [1-2]. Kuo-chih Chou et al. [3-6] had presented a series of methods and calculation formulae of calculating activities from binary phase diagrams. Ying [7-8] and Li [9] had validated systematically the feasibility of these methods. Their results show that the methods of calculating activities from simple eutectic phase diagrams, phase diagrams containing solid solution and involving two liquid phase are quite efficient, and the effectiveness of method is relatively poor for phase diagrams involving intermediate compounds. However, the phase diagrams used by Ying are all complete and relatively simple. Some methods of calculating activity in limited concentration range had been mentioned in Li's study, but those were not suitable for most of binary slag systems. Since the melting point of components are higher, most of the binary phase diagrams of oxide are incomplete, such as CaO-TiO_2 and MgO-TiO_2 [10] systems, and most of them are so complex that there are more types of equilibrium. And even for a complete phase diagram, not only some thermodynamic data are not applicable at higher temperatures, but also a larger error will be caused due to too much the types of equilibrium in calculating the component activity of whole concentration range (mole fraction: 0~1). Simultaneously, the calculation results are inevitably influenced by integral divergence of the formulae near the concentration of stable compound formation. Therefore, these problems must be considered and solved. However, there are no studies about the solution of above problems in the existing literature. Based on previous studies [11-12], this paper put forward the methods of calculating activities in the limited concentration range from binary

phase diagrams to solve the problems of how to calculate activities from incomplete binary phase diagrams and to avoid the influence of integral divergence near the concentration of stable compound formation, and finally get reliable component activity data of the binary Ti-bearing blast furnace slag systems. The results can provide important basic data for further studying the thermodynamic properties of complex titanium bearing slag system and constructing thermodynamic model with solid physical foundation.

2. Calculation Method

2.1. Formulae of Calculating Activities from Binary Phase Diagrams

A series of formulae of calculating component activities from different types of phase diagrams had been derived by Kuo-chih Chou [3-6] using the Gibbs-Duhem equation and relationship between activity coefficient and temperature. The relationship between activity coefficient and temperature as shown in Eq.(1).

$$\sigma_0 \ln \gamma_{i,T_0} = \sigma \ln \gamma_{i,T} \tag{1}$$

Where $\gamma_{i,T0}$, $\gamma_{i,T}$ are activity coefficients of component *i* relative to pure substance at temperature T_0 and T, respectively; $\sigma=T/(1-T/\theta)$, $\sigma_0=T_0/(1-T_0/\theta)$. The activity data are calculated in this study under the condition of regular solution's assumption, namely, $\theta=\infty$, $\sigma=T$ and $\sigma_0=T_0$. In order to convenient writing, we use subscripts "1" and "2" to represent left and right component in phase diagram, respectively. The formulae of different types of phase diagrams are as following:

2.1.1. Equilibrium between liquid solution and pure solid phase [3]

In the concentration range of solid phase equilibrium between the left end of eutectic point and pure component "1" at T_0 temperature, the calculation formula of activity coefficient of each component is:

$$\mathrm{d}\ln\gamma_{1,T_0} = \frac{\Delta_{fus}S^{\Theta}_{m1}(T) - \Delta_{fus}H^{\Theta}_{m1}(T)/\theta}{R}\mathrm{d}(\frac{\sigma}{\sigma_o}) - \mathrm{d}(\frac{\sigma}{\sigma_o}\ln x_1) \tag{2}$$

$$\mathrm{d}\ln\gamma_{2,T_0} = \frac{1}{x_2}[\frac{x_1}{R}(\frac{\Delta_{fus}H^{\Theta}_{m1}(T)}{\theta} - \Delta_{fus}S^{\Theta}_{m1}(T)) + \sum X]\mathrm{d}(\frac{\sigma}{\sigma_o}) - \mathrm{d}(\frac{\sigma}{\sigma_o}\ln x_2) \tag{3}$$

In the concentration range of solid phase equilibrium between the right end of eutectic point and pure component "2" at T_0 temperature, the calculation formula of activity coefficient of each component is:

$$\mathrm{d}\ln\gamma_{1,T_0} = \frac{1}{x_1}[\frac{x_2}{R}(\frac{\Delta_{fus}H^{\Theta}_{m2}(T)}{\theta} - \Delta_{fus}S^{\Theta}_{m2}(T)) + \sum X]\mathrm{d}(\frac{\sigma}{\sigma_o}) - \mathrm{d}(\frac{\sigma}{\sigma_o}\ln x_1) \tag{4}$$

$$\mathrm{d}\ln\gamma_{2,T_0} = \frac{\Delta_{fus}S^{\Theta}_{m2}(T) - \Delta_{fus}H^{\Theta}_{m2}(T)/\theta}{R}\mathrm{d}(\frac{\sigma}{\sigma_o}) - \mathrm{d}(\frac{\sigma}{\sigma_o}\ln x_2) \tag{5}$$

Where, $\sum X=x_1\ln x_1+x_2\ln x_2$; $\Delta_{fus}H^{\Theta}_{mi}(T)$, $\Delta_{fus}S^{\Theta}_{mi}(T)$ are the standard molar melting enthalpy and standard molar melting entropy of component *i* ("1" or "2") at temperature *T*, respectively.

2.1.2. Equilibrium between liquid solution and solid phase of compound [4]

The formulae of calculating component activity coefficients in the concentration range of solution balanced with solid of compound "1_m2_n" at a fixed temperature T_0 are as follows:

$$\mathrm{d}\ln\gamma_{1,T_0}=\frac{-1}{mx_2-nx_1}[\frac{x_2(\Delta_rS_m^{\Theta}(T)-\Delta_rH_m^{\Theta}(T)/\theta)}{R}+n\sum X]\mathrm{d}(\frac{\sigma}{\sigma_o})-\mathrm{d}(\frac{\sigma}{\sigma_o}\ln x_1) \tag{6}$$

$$\mathrm{d}\ln\gamma_{2,T_0}=\frac{1}{mx_2-nx_1}[\frac{x_1(\Delta_rS_m^{\Theta}(T)-\Delta_rH_m^{\Theta}(T)/\theta)}{R}+m\sum X]\mathrm{d}(\frac{\sigma}{\sigma_o})-\mathrm{d}(\frac{\sigma}{\sigma_o}\ln x_2) \tag{7}$$

Where, $\sum X=x_1\ln x_1+x_2\ln x_2$; $\Delta_rH_m^{\Theta}(T)$, $\Delta_rS_m^{\Theta}(T)$ are the standard molar reaction enthalpy and entropy of following combination reaction (8) at temperature T, respectively.

$$m\,1\,(\text{liquid})+n\,2\,(\text{liquid})=1_m2_n\,(\text{solid}) \tag{8}$$

It can be seen from Eqs.(6) and (7) that when the concentration is at the formation concentration of stable compounds, the numerical integration will diverge, that is $\mathrm{d}\ln\gamma_{i,T0}\to\infty$.

2.1.3. Equilibrium between liquid solution and solid solution [5]

The formulae of calculating component activity coefficients in the concentration range of liquid solution balanced with solid solution at a fixed temperature T_0 are as follows:

$$\mathrm{d}\ln r_1^l(T_0)=\frac{x_2^l}{x_2^s-x_2^l}[x_1^s\mathrm{d}(\frac{\sigma}{\sigma_0}\frac{\Delta_{fus}G_{m1}^{\Theta}(T)}{RT})+x_2^s\mathrm{d}(\frac{\sigma}{\sigma_0}\frac{\Delta_{fus}G_{m2}^{\Theta}(T)}{RT})+x_1^s\mathrm{d}(\frac{\sigma}{\sigma_0}\ln\frac{x_1^l}{x_1^s})+x_2^s\mathrm{d}(\frac{\sigma}{\sigma_0}\ln\frac{x_2^l}{x_2^s})] \tag{9}$$

$$\mathrm{d}\ln r_2^l(T_0)=\frac{x_1^l}{x_1^s-x_1^l}[x_1^s\mathrm{d}(\frac{\sigma}{\sigma_0}\frac{\Delta_{fus}G_{m1}^{\Theta}(T)}{RT})+x_2^s\mathrm{d}(\frac{\sigma}{\sigma_0}\frac{\Delta_{fus}G_{m2}^{\Theta}(T)}{RT})+x_1^s\mathrm{d}(\frac{\sigma}{\sigma_0}\ln\frac{x_1^l}{x_1^s})+x_2^s\mathrm{d}(\frac{\sigma}{\sigma_0}\ln\frac{x_2^l}{x_2^s})] \tag{10}$$

Where, $\Delta_{fus}G_{mi}^{\Theta}(T)$ indicate the standard molar melting Gibbs free energy of fusion of component i ("1" or "2") at temperature T; x_i^l , x_i^s are the mole fractions of component i ("1" or "2") at corresponding liquidus and solidus, respectively.

2.2. Solving Method of Differential Equation

In this research, Gauss Legendre numerical integration method is used to solve Eq.(2) to Eq.(10) differential equations. Since the temperature in the binary phase diagram can be expressed as a formula about composition, the integrand function is uniformly expressed as a formula only related to x_2 and then numerical integration calculation is carried out. The specific steps are as follows:

Step 1: By fitting the liquidus of phase diagram, the functions $T(x_2)$ of the temperature on the liquidus with respect to the concentration variable x_2 can be obtained.

Step 2: By fitting the solidus of solid solution of phase diagram, the function $x_{2s}(x_2)$ of the concentration x_{2s} of the solidus with respect to the concentration variable x_2 can be obtained.

Step 3: The univariate differential equation of component activity coefficient with respect to concentration x_2 can be obtained by bringing the fitting results into the corresponding formula.

Step 4: After the integral initial value is determined, the activity coefficients and activity values of each component in a certain temperature and concentration range can be calculated by Gauss Legendre method.

For the incomplete phase diagram, how to determine the initial value of integration is the key to realize the activity calculation. For phase diagrams containing stable compounds, how to avoid

integral divergence near the formation concentration of compounds is the key to improve the accuracy of activity calculation. Based on the previous research, a new method to obtain the initial value of integration is proposed, and the calculation method of component activity in the limited concentration range from the incomplete phase diagram is obtained.

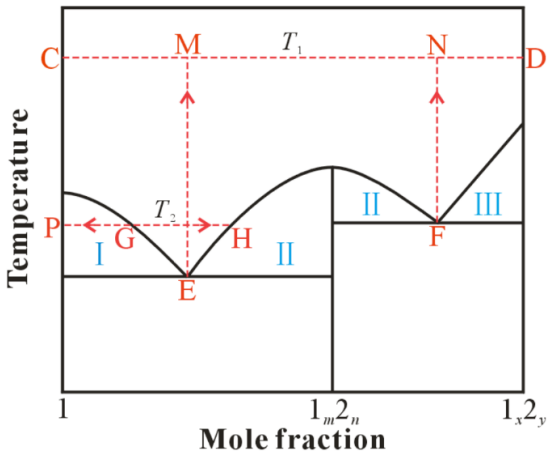

Figure 1. The representative phase diagram involving tow intermediate compounds

Fig.1 shows a simplified 1-2 binary phase diagram involving a simple eutectic and two compounds. The equilibrium relationships of each region in Fig.1 are as follows:

Region I: Equilibrium between liquid solution and pure solid of component "1", satisfy the following relationship:

$$\Delta_{fus}G^{\Theta}_{m1}(T) = -RT\ln a_{1(l,l)} \tag{11}$$

Region II: Equilibrium between liquid solution and solid phase of compound "1_m2_n", satisfy the following relationship:

$$\Delta_{r1}G^{\Theta}_{m}(T) = RT\ln a^{m}_{1(l,l)}a^{n}_{2(l,l)} \tag{12}$$

Region III: Equilibrium between liquid solution and solid phase of compound "1_x2_y", satisfy the following relationship:

$$\Delta_{r2}G^{\Theta}_{m}(T) = RT\ln a^{x}_{1(l,l)}a^{y}_{2(l,l)} \tag{13}$$

Where, $a_{i(l,l)}$ is activity of component i ("1" or "2") relative to pure liquid i in solution; $\Delta_{r1}G^{\Theta}_{m}(T)$ and $\Delta_{r2}G^{\Theta}_{m}(T)$ are the standard molar reaction Gibbs free energies of the formation reactions of compounds "1_m2_n" and "1_x2_y", respectively.

Steps for calculating the each component activity of PH section in Fig.1:

Step 1: The activity of component "1" at point G, $a_{1,G}$, can be calculated by Eq.(11).

Step 2: Taking $a_{1,G}$ as a initial value of numerical integration, the activities of component "1" at segment GH can be obtained by using Eq.(2). Meanwhile, we can get the activity of component "1" at point H, $a_{1,H}$.

Step 3: The activity of component "2" at point H, $a_{2,H}$, can be calculated by Eq.(12).

Step 4: Taking $a_{2,H}$ as a initial value of numerical integration, the activities of component "2" at segment GH can be obtained by using Eq.(3).

Step 5: According to the phase equilibrium relationship in region I and the binary Gibbs-Duhem equation, $x_1\mathrm{d}\ln a_1+x_2\mathrm{d}\ln a_2=0$, it can be obtained that the component activity relationship in PG section

is $a_{1,PG}$=$a_{1,G}$=constant value and $a_{2,PG}$=$a_{2,G}$=constant value. Then, the each component activities at whole segment PH have been calculated.

As shown in Fig.1, point E is the intersection of region I and region II, then the activities of each component at this point simultaneously satisfy Eq.(11) and Eq.(12), and point F is the intersection of region II and region III, then the activities of each component at this point simultaneously satisfy Eq.(12) and Eq.(13). Combining the above formulas, we have

$$\begin{cases} \Delta_{fus} G_{m1}^{\Theta}(T) = -RT \ln a_{1(l,l)} \\ \Delta_{r1} G_{m}^{\Theta}(T) = RT \ln a_{1(l,l)}^{m} a_{2(l,l)}^{n} \end{cases} \tag{14}$$

$$\begin{cases} \Delta_{r1} G_{m}^{\Theta}(T) = RT \ln a_{1(l,l)}^{m} a_{2(l,l)}^{n} \\ \Delta_{r2} G_{m}^{\Theta}(T) = RT \ln a_{1(l,l)}^{x} a_{2(l,l)}^{y} \end{cases} \tag{15}$$

Steps for calculating the each component activity of CD section in Fig.1:

Step 1: The activity of each component at point E or F, $a_{i,E}$ or $a_{i,F}$, can be calculated by solving Eq.(14) or Eq.(15), respectively.

Step 2: The activity of each component at point M or N, $a_{i,M}$ or $a_{i,N}$, can be obtained by Eq.(1).

Step 3: Taking $a_{i,M}$ or $a_{i,N}$, as a initial value of numerical integration, the activities of each component at segments MC, ND or whole segment CD can be obtained by using Eq.(2) to Eq.(7).

Through the study of Kuo Chih Chou formula, it is found that the activity of component in liquid solution calculated by the formula is referred to pure liquid phase. Therefore, according to different applications, the activity standard state can be converted according to Eq.(16).

$$\Delta_{fus} G_{mi}^{\Theta}(T) = -RT \ln \frac{a_{i(l,l)}}{a_{i(l,s)}} = -RT \ln \frac{\gamma_{i(l)}}{\gamma_{i(s)}} \tag{16}$$

Where $a_{i(l,s)}$ is activity of component i relative to pure solid i in liquid solution; $\gamma_{i(l)}$ is activity coefficient of component i relative to pure liquid i in liquid solution; $\gamma_{i(s)}$ is activity coefficient of component i relative to pure solid i in liquid solution.

If we apply above methods flexibly in conventional computation procedure, it can effectively reduce the calculation errors, avoid the effect of integral divergence near the concentration of stable compound formation and extend the applying range of calculating activities from binary phase diagrams of slag system.

3. Calculation Results and Discussion

3.1. Acquisition of thermodynamic data

The basic thermodynamic data required in this paper are found in reference [10]. The enthalpy and entropy used in the formula are calculated by Kirchhoff's laws, and the Gibbs free energy is calculated from the formula $\Delta G(T)=\Delta H(T)–T\Delta S(T)$. The results are shown in Tables 1 and 2.

Table 1. The fusion thermodynamic properties of components

Component *i*	$\Delta_{fus}H_{mi}^{\Theta}(T)$, $\Delta_{fus}S_{mi}^{\Theta}(T)$
Al_2O_3	$\Delta_{fus}H_{Al_2O_3}^{\Theta}=88717-4.8367\times10^{6}/T+24.347T-4.596\times10^{-3}T^{2}$
	$\Delta_{fus}S_{Al_2O_3}^{\Theta}=-116.03-2.4184\times10^{6}/T^{2}-9.192\times10^{-3}T+24.347\ln T$
CaO	$\Delta_{fus}H_{CaO}^{\Theta}=60639-6.9450\times10^{5}/T+13.138T-2.2595\times10^{-3}T^{2}$
	$\Delta_{fus}S_{CaO}^{\Theta}=-64.067-3.4725\times10^{5}/T^{2}-4.5190\times10^{-3}T+13.138\ln T$
MgO	$\Delta_{fus}H_{MgO}^{\Theta}=56538-0.11422\times10^{7}/T+11.715T-0.1569\times10^{-2}T^{2}$
	$\Delta_{fus}S_{MgO}^{\Theta}=-59.404-0.5711\times10^{6}/T^{2}-0.3138\times10^{-2}T+11.715\ln T$
MnO	$\Delta_{fus}H_{MnO}^{\Theta}=42569-3.682\times10^{5}/T+14.184T-4.0585\times10^{-3}T^{2}$
	$\Delta_{fus}S_{MnO}^{\Theta}=-65.04-1.841\times10^{5}/T^{2}-8.117\times10^{-3}T+14.184\ln T$
SiO_2	$\Delta_{fus}H_{Cristobalite}^{\Theta}=-12940-3.9037\times10^{6}/T+14.142T-9.4150\times10^{-4}T^{2}$
	$\Delta_{fus}S_{Cristobalite}^{\Theta}=-98.416-1.9518\times10^{6}/T^{2}-1.8830\times10^{-3}T+14.142\ln T$
	$\Delta_{fus}H_{Tridymite}^{\Theta}=-26908+28.702T-5.5230\times10^{-3}T^{2}$
	$\Delta_{fus}S_{Tridymite}^{\Theta}=-192.51-1.1046\times10^{-2}T+28.702\ln T$
TiO_2	$\Delta_{fus}H_{TiO_2}^{\Theta}=39828-9.958\times10^{5}/T+25.02T-5.6695\times10^{-3}T^{2}$
	$\Delta_{fus}S_{TiO_2}^{\Theta}=-136.25-4.979\times10^{5}/T^{2}-0.0113T+25.02\ln T$

Table 2. The thermodynamic properties of formation of compounds

Compound	$\Delta_rH_m^{\Theta}(T)$, $\Delta_rS_m^{\Theta}(T)$
$Al_2O_3.TiO_2$	$\Delta_rH_{AT}^{\Theta}=-1.3038\times10^{5}+4.6903\times10^{6}/T-50.179T+0.0111T^{2}$
	$\Delta_rS_{AT}^{\Theta}=269.73+2.3452\times10^{6}/T^{2}+0.0222T-50.179\ln T$
$CaO.SiO_2$	$\Delta_rH_{CS,Tridymite}^{\Theta}=-1.3958\times10^{5}-14.644T-4.3368\times10^{-19}T^{2}$
	$\Delta_rS_{CS,Tridymite}^{\Theta}=83.244-8.6736\times10^{-19}T-14.644\ln T$
	$\Delta_rH_{CS,Cristobalite}^{\Theta}=-1.4012\times10^{5}-14.644T-5.4210\times10^{-19}T^{2}$
	$\Delta_rS_{CS,Cristobalite}^{\Theta}=81.749-50/T^{2}-1.0842\times10^{-18}T-14.644\ln T$
$2CaO.SiO_2$	$\Delta_rH_{C_2S}^{\Theta}=-2.4820\times10^{5}-6.2760T-9.7578\times10^{-19}T^{2}$
	$\Delta_rS_{C_2S}^{\Theta}=12.160-50/T^{2}-1.9516\times10^{-18}T-6.2760\ln T$
$MgO.SiO_2$	$\Delta_rH_{MS}^{\Theta}=-75292-24.016T-0.10842\times10^{-18}T^{2}$
	$\Delta_rS_{MS}^{\Theta}=147.23-50/T^{2}-0.21684\times10^{-18}T-24.016\ln T$
$2MgO.SiO_2$	$\Delta_rH_{M_2S}^{\Theta}=-0.15464\times10^{6}-53.179T+0.38493\times10^{7}/T+0.01182T^{2}$
	$\Delta_rS_{M_2S}^{\Theta}=306.33+0.19246\times10^{7}/T^{2}+0.023640T-53.179\ln T$
$2MgO.TiO_2$	$\Delta_rH_{M_2T}^{\Theta}=-0.16751\times10^{6}+0.30501\times10^{7}/T-56.861T+0.017008T^{2}$
	$\Delta_rS_{M_2T}^{\Theta}=310.26+0.15250\times10^{7}/T^{2}+0.034016T-56.861\ln T$
$MgO.TiO_2$	$\Delta_rH_{MT}^{\Theta}=-0.12561\times10^{6}+0.27865\times10^{7}/T-29.999T+0.67780\times10^{-2}T^{2}$
	$\Delta_rS_{MT}^{\Theta}=151.09+0.13932\times10^{7}/T^{2}+0.013556T-29.999\ln T$
$MgO.2TiO_2$	$\Delta_rH_{MT_2}^{\Theta}=-0.1541\times10^{6}+0.31296\times10^{7}/T-65.982T+0.019183T^{2}$
	$\Delta_rS_{MT_2}^{\Theta}=360.26+0.15648\times10^{7}/T^{2}+0.038367T-65.982\ln T$
$2MnO.TiO_2$	$\Delta_rH_{M_2T}^{\Theta}=-1.6945\times10^{5}+2.5564\times10^{6}/T-41.045T+8.7025\times10^{-3}T^{2}$
	$\Delta_rS_{M_2T}^{\Theta}=193.86+1.2782\times10^{6}/T^{2}+0.0174T-41.045\ln T$
$MnO.TiO_2$	$\Delta_rH_{MT}^{\Theta}=-1.1433\times10^{5}+2.1882\times10^{6}/T-26.861T+4.6440\times10^{-3}T^{2}$
	$\Delta_rS_{MT}^{\Theta}=125.05+1.0941\times10^{6}/T^{2}+92.88T-26.861\ln T$

3.2. Calculation results

The phase diagram [13] of CaO-SiO_2 system is shown in Fig.2. The each component activities at segment AB in CaO-SiO_2 phase diagrams were calculated by the proposed method, and compared with the experimental values. The results are shown in Fig.5. For the component SiO_2, the average

relative error between calculated values by this work and experimental data [13-14] is 17%. For the component CaO, the average relative error between calculated values by this work and experimental data [13] is 21%. Total average relative error is 18%. The phase diagram [13] of MgO-SiO_2 system is shown in Fig.3. The each component activities at segment AB in MgO-SiO_2 phase diagrams were calculated by the proposed method, and compared with the experimental values. The results are shown in Fig.6. For the component SiO_2, the average relative error between calculated values by this work and experimental data [13] is 12%. For the component MgO, the average relative error between calculated values by this work and experimental data [13] is 25%. Total average relative error is 18%. The phase diagram [15] of MnO-TiO_2 system is shown in Fig.4. The each component activities at segment BC in MnO-TiO_2 phase diagrams were calculated by the proposed method, and compared with the experimental values. The results are shown in Fig.7. For the component MnO, the average relative error between calculated values by this work and experimental data [13] is 11%. For the component TiO_2, the average relative error between calculated values by this work and experimental data [13] is 11%. Total average relative error is 11%.

In summary, it can be seen that the application effect of the proposed method in these three systems is better. The calculation error is within the experimental error range of 10%~30% proposed by Turkdogan [16]. The results show that the new methods are feasible in the practical application.

The phase diagrams [13] of Al_2O_3-TiO_2, CaO-TiO_2, MgO-TiO and SiO_2-TiO_2 systems are shown in Fig.8 to Fig11. The component activity data of these binary Ti-bearing blast furnace slag systems at a given temperature and concentration are calculated by the proposed methods. The results are shown in Fig.12 to Fig.18. The relative errors for these systems are comparable to the results of CaO-SiO_2, MgO-SiO_2 and MnO-TiO_2 systems. So the activity data obtained can be used as basic data for thermodynamic study of Ti-bearing blast furnace slag.

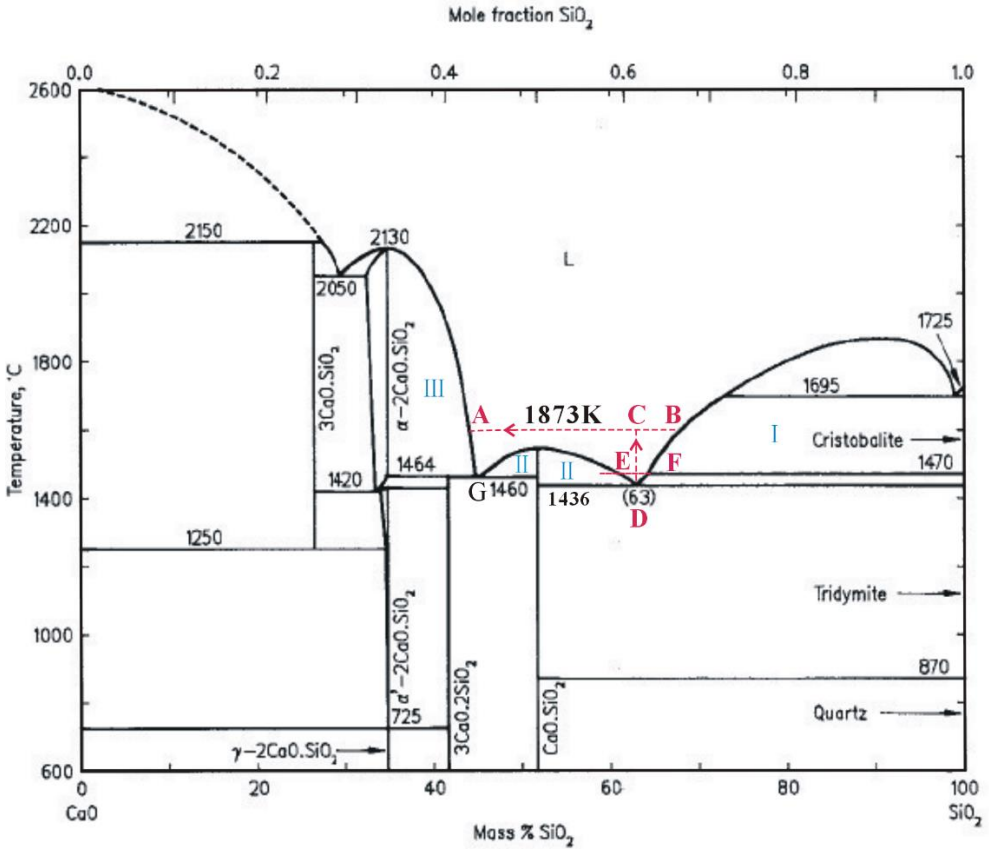

Figure 2. CaO-SiO_2 phase diagram [13]

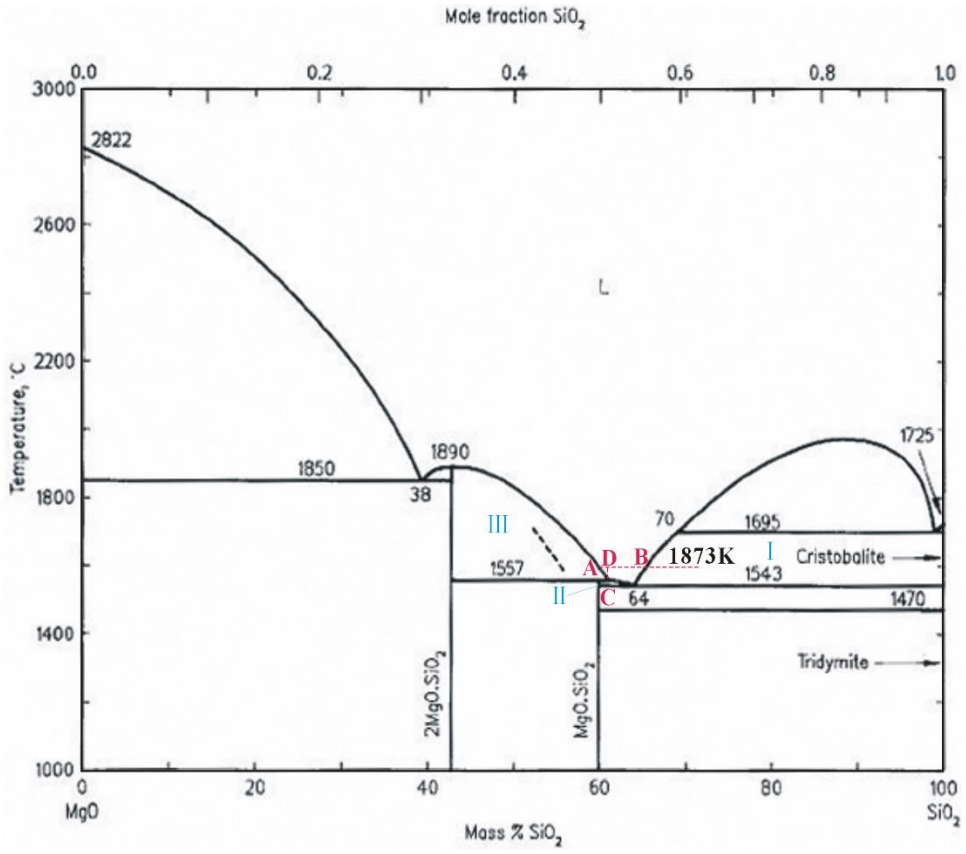

Figure 3. MgO-SiO_2 phase diagram [13]

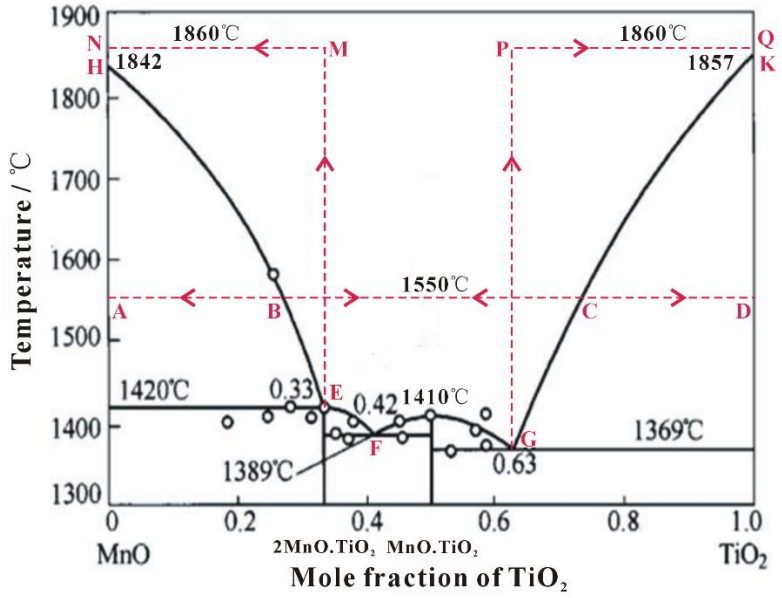

Figure 4. MnO-TiO_2 phase diagram [15]

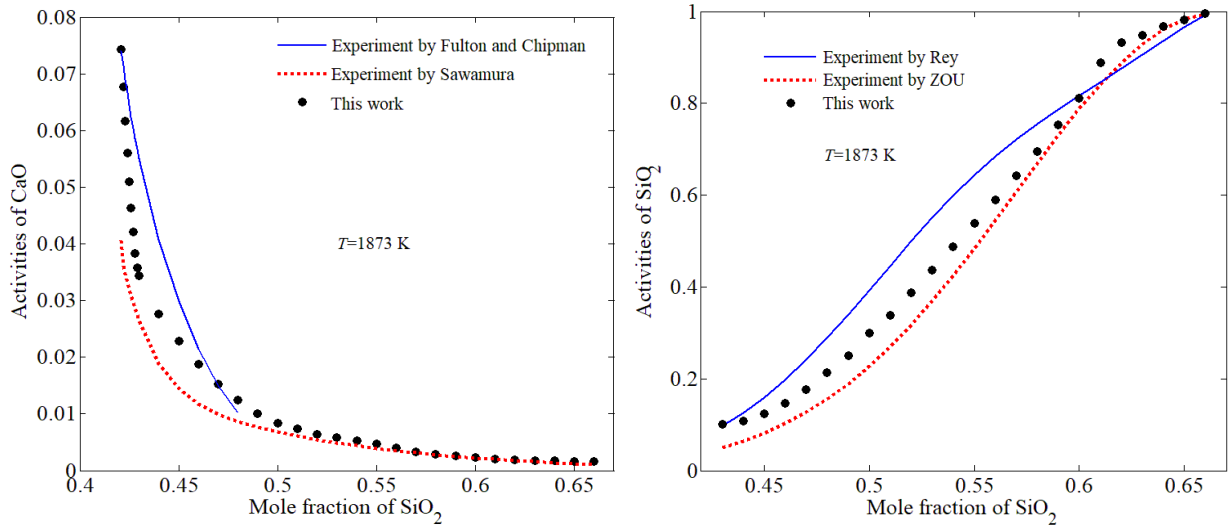

Figure 5. Comparison of calculated by proposed method and experimental activities [13-14] of components CaO and SiO_2 in the CaO-SiO_2 melt at 1873K (Activities are referred to pure solid CaO or solid SiO_2)

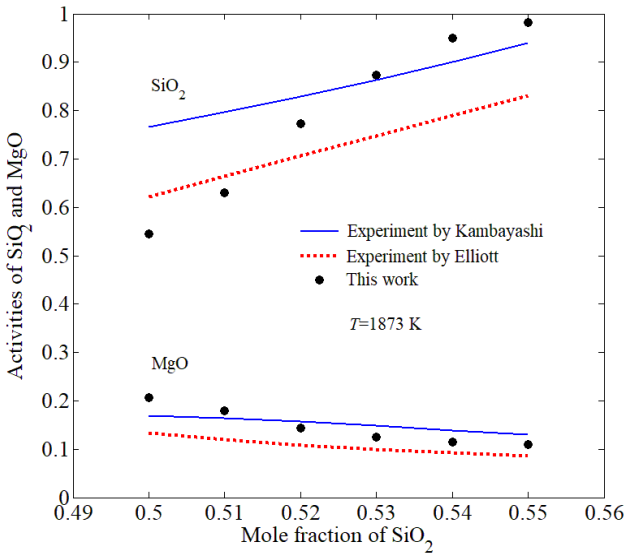

Figure 6. Comparison of the calculated by proposed method and experimental activities [13] of components MgO and SiO_2 in the MgO-SiO_2 melt at 1873K (Activities are referred to pure solid MgO or solid SiO_2)

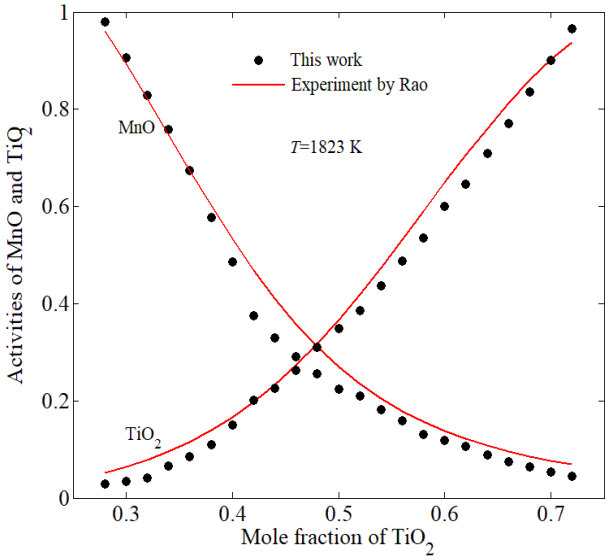

Figure 7. Comparison of calculated by proposed method and experimental activities [13]of components MnO and TiO_2 in the MnO-TiO_2 melt at 1823 K (Activities are referred to pure solid MnO or solid TiO_2)

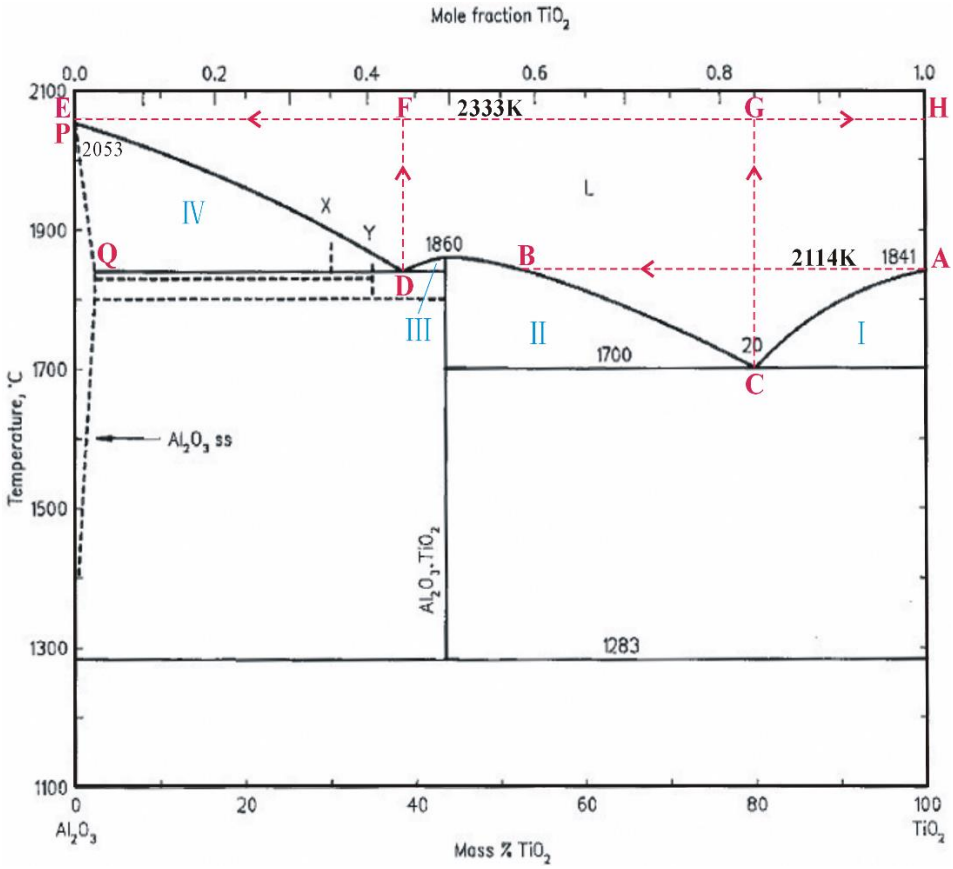

Figure 8. Al_2O_3-TiO_2 phase diagram [13]

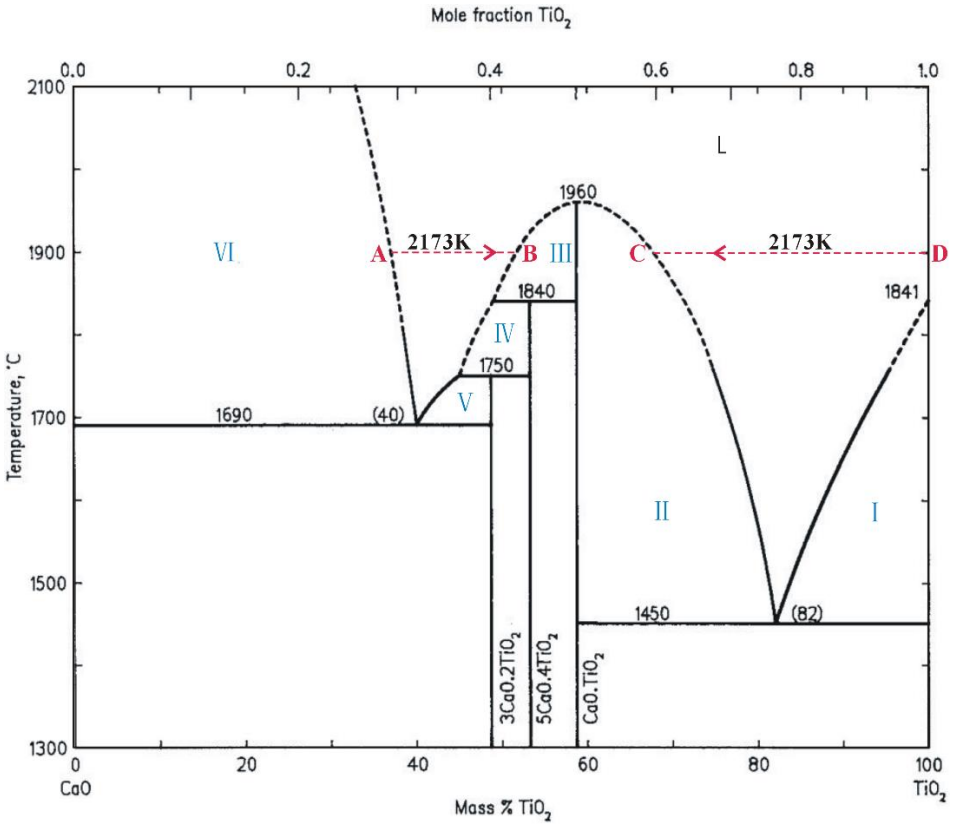

Figure 9. CaO-TiO_2 phase diagram [13]

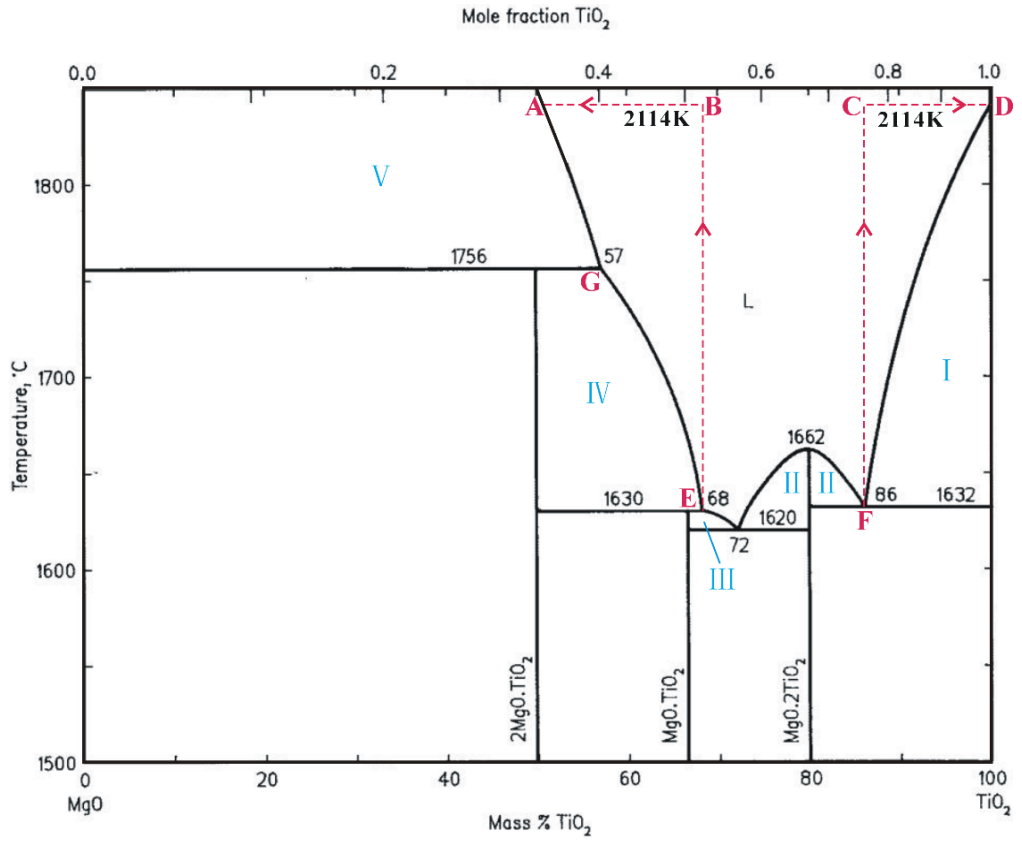

Figure 10. MgO-TiO_2 phase diagram [13]

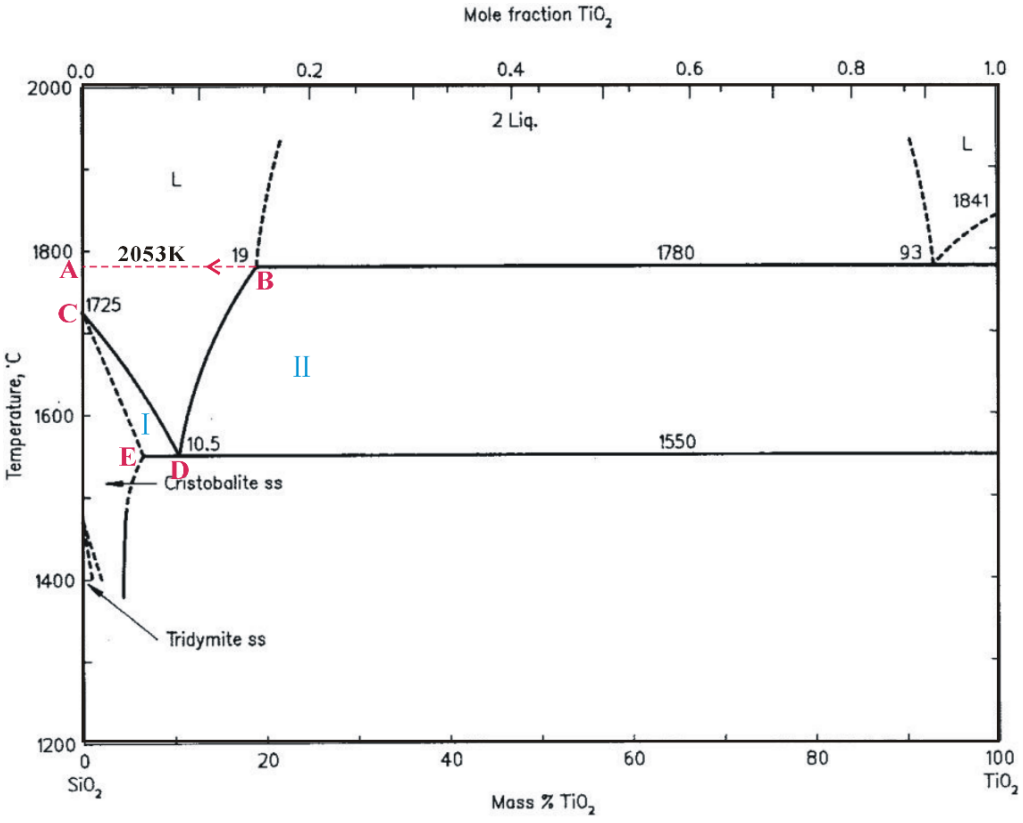

Figure 11. SiO_2-TiO_2 phase diagram [13]

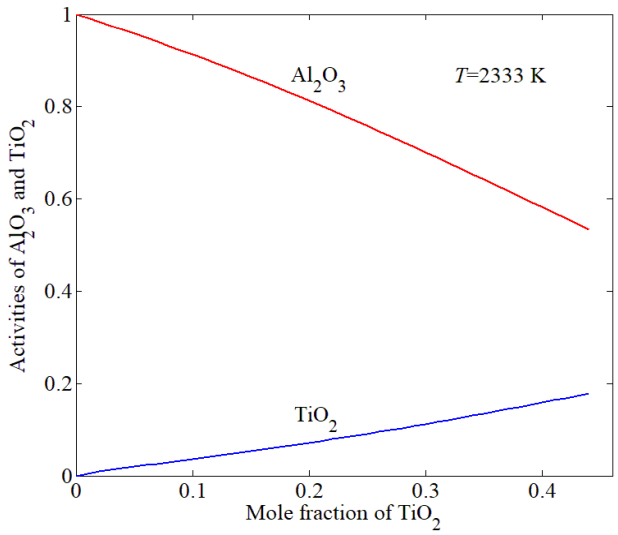

Figure 12. Calculated activities of Al_2O_3 and TiO_2 in segment EF of Al_2O_3-TiO_2 phase diagram (Activities are referred to pure solid Al_2O_3 or liquid TiO_2)

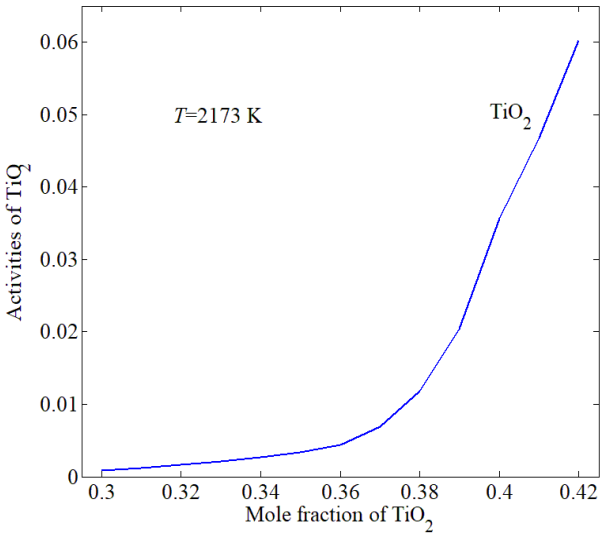

Figure 13. Calculated activities of Al_2O_3 and TiO_2 in segment AB of Al_2O_3-TiO_2 phase diagram (Activities are referred to pure liquid Al_2O_3 or liquid TiO_2)

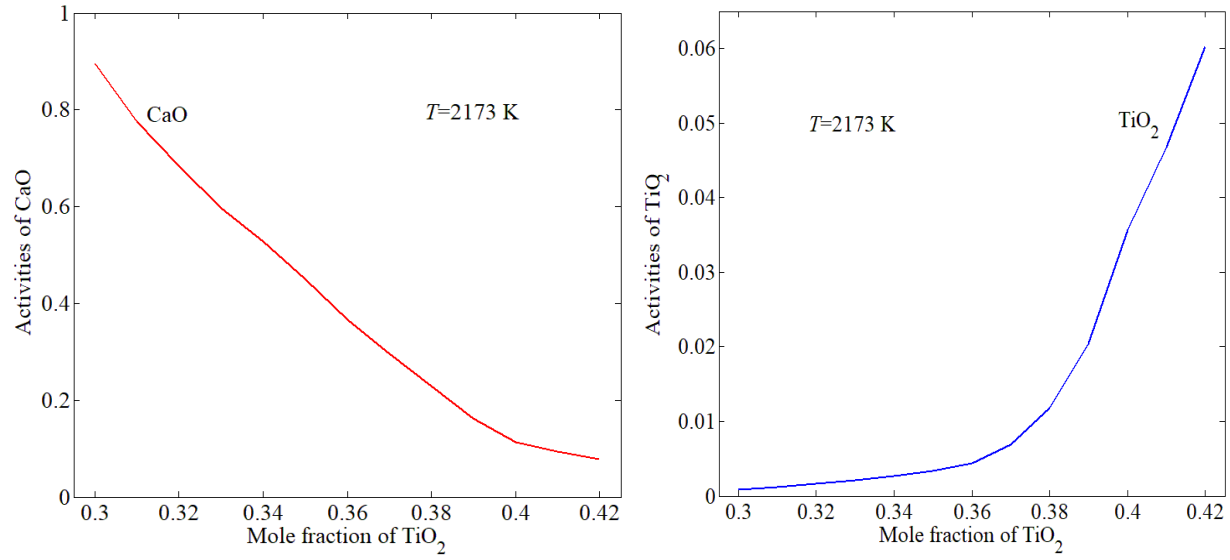

Figure 14. Calculated activities of CaO and TiO_2 in segment AB of CaO-TiO_2 phase diagram (Activities are referred to pure solid CaO or liquid TiO_2)

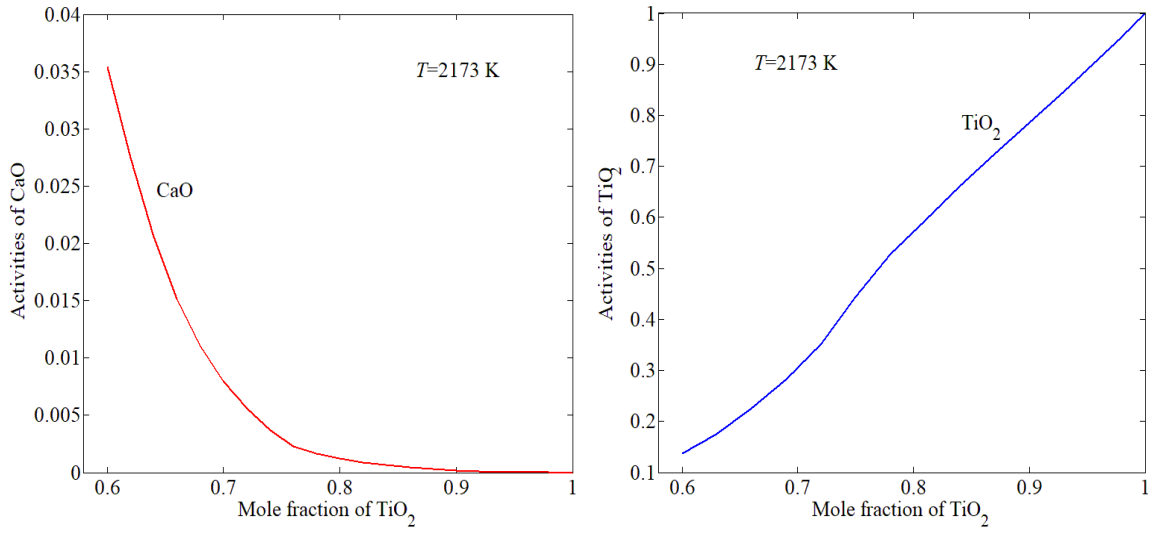

Figure 15. Calculated activities of CaO and TiO_2 in segment CD of CaO-TiO_2 phase diagram (Activities are referred to pure solid CaO or liquid TiO_2)

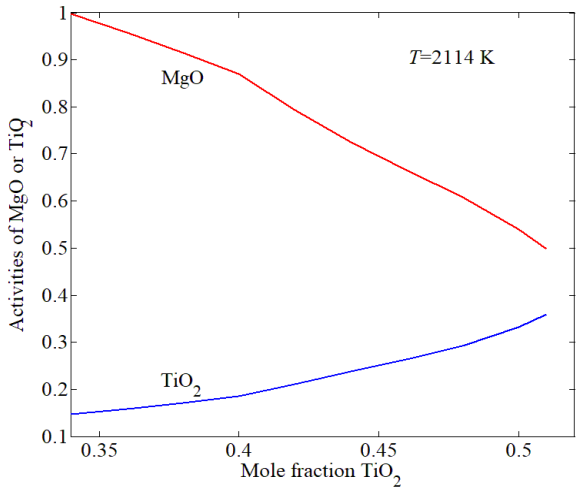

Figure 16. Calculated activities of MgO and TiO_2 in segment AB of MgO-TiO_2 phase diagram (Activities are referred to pure solid MgO or liquid TiO_2)

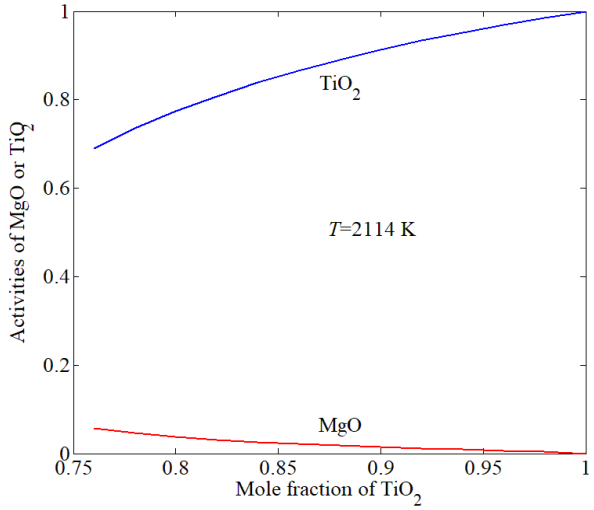

Figure 17. Calculated activities of MgO and TiO_2 in segment CD of MgO-TiO_2 phase diagram (Activities are referred to pure solid MgO or liquid TiO_2)

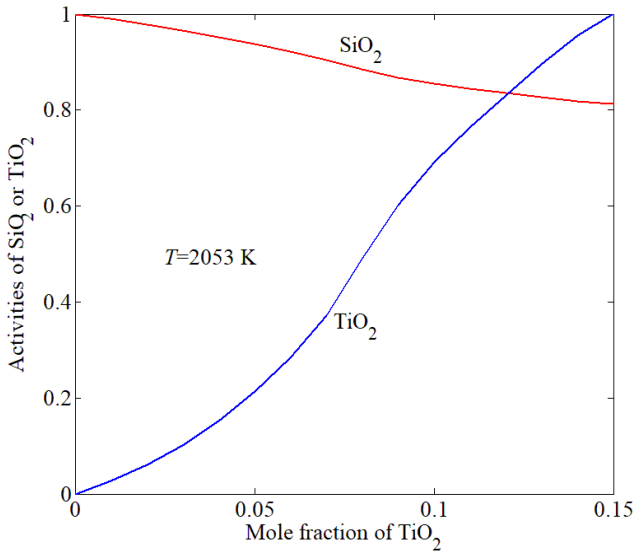

Figure 18. Calculated activities of SiO_2 and TiO_2 in segment AB of SiO_2-TiO_2 phase diagram (Activities are referred to pure liquid SiO_2 or solid TiO_2)

3.3. Analysis and discussion

TiO_2 is an amphoteric oxide, which can be acidic or alkaline in slag. According to ion theory, when TiO_2 is acidic [17]:

$$TiO_2 + (n-2)O^{2-} = TiO_n^{2(n-2)-} \tag{17}$$

When TiO_2 is alkaline [17]:

$$TiO_2 = Ti^{4+} + 2O^{2-} \tag{18}$$

As shown in Figs.7, 14, 15 and 16, CaO, MnO and MgO have strong negative deviation effect on TiO_2. Because CaO, MnO and MgO are alkaline oxides, their existence can increase the activity of oxygen ions in the melt and make TiO_2 acidic in the melt. As shown in Figs.12 and 13, Al_2O_3 has a small negative deviation effect on TiO_2. In this environment, it is considered that Al_2O_3 is more likely to be alkaline. Its existence increases the activity of oxygen ions in the melt, making TiO_2 acidic in melt. As shown in Fig.18, in the high SiO_2 concentration range, SiO_2 has a strong positive deviation effect on TiO_2. Since SiO_2 is an acidic oxide, its existence reduces the activity of oxygen ions in the melt, making TiO_2 alkaline in the high concentration SiO_2 melt. It can be seen that the calculated results are consistent with the actual law.

In conclusion, using phase diagram to obtain the required thermodynamic data is an effective and feasible way when lack of experimental data, which provides important basic data for further studying the thermodynamic properties of complex titanium bearing slag system and building a thermodynamic model with solid physical foundation.

4. Conclusion

Based on the accuracy and feasibility of Kuo-chih Chou formulae as well as the former researches, the methods are proposed to improve numerical integration of these formulae. By using the new methods flexibly, the problem of how to calculate activities from incomplete binary phase diagrams is solved, and the effect of the integral divergence near the concentration of stable compound formation is avoided effectively. Therefore, the calculation errors are reduced at some extent. The component activity data of CaO-SiO_2, MgO-SiO_2 and MnO-TiO_2 melts are calculated by the methods presented under the condition of regular solution's assumption. The calculated results are in reasonable agreement with experimental data, and the average relative errors between calculated values and experimental data are all lower than 20%. The results indicate that the new methods are

feasible. The component activity data of $CaO-TiO_2$, $Al_2O_3-TiO_2$, SiO_2-TiO_2 and $MgO-TiO_2$ melts are calculated by using flexibly the proposed method under the condition of regular solution's assumption, and the relative errors of these systems are comparable to the results of $CaO-SiO_2$, $MgO-SiO_2$ and $MnO-TiO_2$ systems. Therefore, the calculated activities of these four systems are reliable, and they can be used as fundamental data for thermodynamic study of Ti-bearing blast furnace slag. There are important scientific significance to perfecting vanadium titano-magnetite's blast-furnace smelting theory.

Acknowledgments

This work was financially supported by school level scientific research fund project of Kunming metallurgical College (2016xjzk03).

Corresponding author: Zhennan Liu.

References

[1] Z. N. LIU, C.L. Yao, J.H. Hou, et. al. Thermodynamic analysis of Ti (C, N) formation conditions in blast furnace hearth. Mining and Metallurgy, 30 (2021): 85 - 94.

[2] Z. N. LIU, D.P. TAO, C.L. YAO, et. al. Prediction of Component Activity of Titanium Bearing Slag System by M-MIVM. Iron and Steel, 55 (2020): 16 - 29+46.

[3] F. ZHANG, K.C. CHOU, et. al. A new Treatment for calculating activities from a simple eutectic phase diagram. CALPHAD, 16 (1992): 261 - 268.

[4] F. ZHANG, K.C. CHOU, et. al. A new treatment for calculating Activities from phase diagrams involving intermediate compounds. CALPHAD, 16 (1992): 269 - 276.

[5] K. C. CHOU. A New Treatment for calculating activities from phase diagrams containing solid solution. CALPHAD, 14 (1990): 275 - 282.

[6] F. ZHANG, K.C. CHOU, et. al. A new treatment for calculating activities from phase diagrams involving two liquid or solid Coextsting phases. CALPHAD, 14 (1990): 349 - 362.

[7] X.Y. YING, D.P. TAO. Systematic validation of methods on calculating activities from binary phase diagrams. Journal of Kunming University of Science and Technology (Natural Science Edition), 4 (2011): 11 - 17.

[8] X. Y. YING, D.P. TAO, H.W. YANG. Calculation of infinite dilute activity coefficients from binary alloy phase diagrams. Journal of Kunming University of Science and Technology (Natural Science Edition), 39 (2014): 1 - 7+54.

[9] Z.Y. LI, D. P. TAO. A System verification of methods on calculating activities from binary slag phase diagrams involving intermediate Compounds. Journal of Kunming University of Science and Technology (Natural Science Edition), 1 (2013): 6 - 11.

[10] D. L. YE, J.H. HU. Handbook of Thermodynamic Data for Applied Inorganic Material 2nd Ed. 2nd Edition, Beijing: Metallurgical Industry Press, 2002.

[11] Z. N. LIU. Study on phase equilibrium between titanium-bearing blast furnace slag and molten iron by using pseudo-multicomponent approach of MIVM. Kunming: Kunming University of Science and Technology. Faculty of Metallurgical and Energy Engineering, (2014): 6 - 87.

[12] Z. N. LIU, D.P. TAO, C.L. YAO, et. al. Calculating activities and infinite dilution activity coefficients from Al2O3-TiO2, MnO-TiO2 and SiO2-TiO2 phase diagrams. Journal of Kunming University of Science and Technology (Natural Science Edition), 43 (2018): 1 - 13.

[13] VDEh. Slag Atlas, 2nd Edition. Germany: Verlag Stahleisen GmbH, 1995.

[14] Y. X. ZOU, J.C. ZHOU et al. Some Aspects of the Thermodynamics of Melts, Acta Metall, 2 (1982): 127 - 140.

[15] J. ZHANG. Thermodynamic calculation of metallurgical melt and solution. Beijing: Metallurgical Industry Press, 2007.

[16] E. T. TURKDOGAN. Physicochemical properties of molten slags and glasses. London, U.K.: The Metals Society, 1983.

[17] Y. MORIZANE, B. OZTURK, R. J. FRUEHAN. Thermodynamics of TiOx in blast furnace-type slags. Metallurgical and Materials Transactions B, 30 (1999): 29 - 43.